

The Indirect Determination of Enzyme Kinetics using Capillary Electrophoresis with
Chemiluminescence Detection

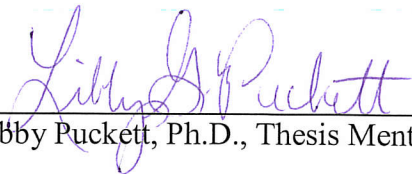
Honors Thesis

By: Gracie Portagallo

A.R. Smith Department of Chemistry and Fermentation Sciences, Appalachian State University,

Boone, NC 28608

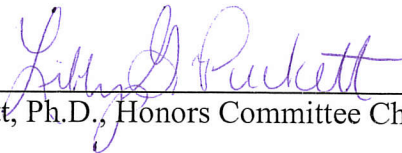
May 2021



Libby Puckett, Ph.D., Thesis Mentor



Carol Babyak, Ph.D., Second Reader



Libby Puckett, Ph.D., Honors Committee Chair



Claudia Cartaya-Marin, Ph.D., Chemistry and
Fermentation Sciences Department Chair

Table of Contents:

Abstract	4
Introduction	5
Capillary Electrophoresis	5
Chemiluminescence Detection	10
Electrophoretically Mediated Microanalysis	11
Materials and Methods	19
Results and Discussion	24
Validation of the instrument: luminol injections	24
Glucose Oxidase Injections	27
Conclusion and Future Work	37
References	38
Vita	41

List of Figures:

Figure 1: Capillary electrophoresis system set-up using an on-column detector	5
Figure 2: EOF diagram in the capillary showing the charged double layer from the cations in the buffer	6
Figure 3: Different types of flow profiles that can occur in a capillary, with responses	8
Figure 4: Chemiluminescence reaction of hydrogen peroxide and luminol	10
Figure 5: Enzyme-Substrate complex binding - Lock and key model (A) and the induced fit model (B)	12
Figure 6: Example of Michaelis-Menten plot (A) and Lineweaver-Burk plot (B)	13
Figure 7: Zone of enzyme in the capillary using EMMA	14
Figure 8: Example of expected EMMA plateau (A), EMMA plateau where excess product is detected first (B), and EMMA plateau where excess product is detected at the end (C)	15
Figure 9: Catalyzed oxidation reaction of β -D-glucose	16
Figure 10: Enzyme inhibition reaction	17
Figure 11: Lineweaver-Burk plots of competitive inhibition (A), noncompetitive inhibition (B), and uncompetitive inhibition (C)	18
Figure 12. Structure of competitive inhibitor (A) and substrate (B)	18
Figure 13: Diagram of the CE-CL system (A) and custom CE system with post-column CL detection (B)	20
Figure 14: Photon counter program used on LabVIEW and EMMA Plateau	21
Figure 15. Normalization of triplicate trials using $1.00 \times 10^{-5} \text{ M}$ (A) and $2.50 \times 10^{-6} \text{ M}$ (B)	25
Figure 16. Normalization of various luminol concentrations used	26

Figure 17: Normalization of various luminol concentrations used (A) and calibration curve (B)	27
Figure 18: Previous results of EMMA plateaus using various glucose oxidase concentrations (A) and the calibration curve (B)	29
Figure 19: Previous results of a Michaelis-Menten plot of glucose oxidase	30
Figure 20: Previous results of a Lineweaver-Burk plot of glucose oxidase	30
Figure 21. Normalization of replicate trials using 25 U glucose oxidase (A) and 50 U glucose oxidase (B)	31
Figure 22: Normalization of EMMA plateaus using various concentrations of glucose oxidase (A) and calibration curve (B)	32
Figure 23. Michaelis-Menten plot of glucose oxidase	33
Figure 24. Lineweaver- Burk plot of glucose oxidase	33
Figure 25. Normalization of luminol injections using $1.00 \times 10^{-5} \text{ M}$ (before changing the cathode)	35
Figure 26: Normalization of EMMA plateaus using 100U of glucose oxidase	35
Figure 27: Normalization of EMMA plateaus using 100U of glucose oxidase (A) and 75 U glucose oxidase (B) (after changing the cathode)	36
List of Equations:	
Equation 1: Velocity of an ion	6
Equation 2: Electrophoretic mobility of an ion	6
Equation 3: Enzyme kinetics	11
Equation 4: Michaelis-Menten equation	12
Equation 5: Lineweaver-Burk plot equation	13

Abstract:

A custom capillary electrophoresis system with post-column chemiluminescence detection (CE-CL) was used with electrophoretically mediated microanalysis (EMMA) to indirectly determine the enzyme kinetics of glucose oxidase. Validation of the instrument was performed through injecting luminol hydrodynamically to measure the consistency of the results, as well as learning how to use the CE-CL system. Based on the results obtained from the luminol injections, there was strong linearity present, with an R^2 value of 0.9925, as the concentration of luminol increased. The glucose oxidase was introduced by electrokinetically injecting the enzyme into the system to react with the substrate, β -D-glucose. The byproduct, hydrogen peroxide, was produced on column and reacted with luminol in the outlet cell, in which the production of light was detected by the photon counter. Based on the results obtained from the glucose oxidase injections, there was a fairly strong linearity present, with an R^2 value of 0.976. As the concentration of glucose oxidase increased, the intensity of the plateaus also increased because there was an increase in the formation of product. CE-CL has been proven to be an effective technique to indirectly determine kinetic constants of enzymes that produce hydrogen peroxide and to be later compared to literature values.

Introduction:*Capillary electrophoresis*

Capillary electrophoresis is a separation technique that is becoming more commonly used because of its speed, efficiency, high sensitivity, small sample volume, minimal waste, as well as its various applications.¹⁻⁴ Capillary electrophoresis does not have a stationary phase, and utilizes a large electric field to carry the solution across the capillary and results in separation based on charge from the generation of electroosmotic flow. A typical capillary electrophoresis system, which is shown in Figure 1, consists of an anode in an inlet buffer and a cathode in an outlet buffer solution. Both buffers contain the capillary and are connected to a high voltage power supply, and the detector cell is on-column.¹ In the set-up used for this experimentation, the detection cell contains an optical window for post-column detection rather than an on-column detection window.

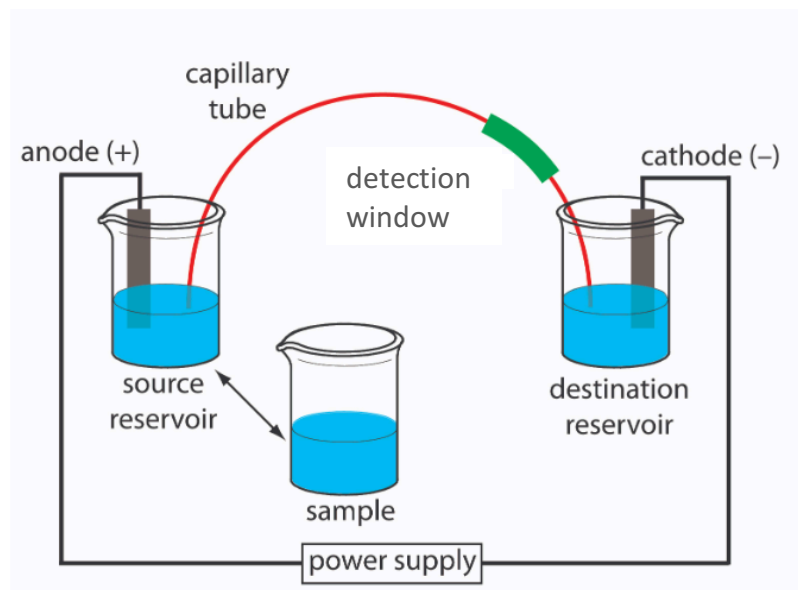


Figure 1. Capillary electrophoresis system set-up using an on-column detector.⁵

Electroosmotic flow (EOF) causes the solution to travel across the capillary from the anode to the cathode.¹ In order for this to occur, the capillary has to be washed first with sodium

hydroxide, which deprotonates the silanol groups of the fused silica capillary. Then, the cations in the buffer form a charged double layer, which is shown in Figure 2. This process allows the cations in the solution to flow from the anode to cathode when a potential is applied.¹ Cations travel the fastest, because they are attracted to the cathode, while the neutral charges are moved because of EOF, and the anions travel the slowest because of their attraction to the anode, but will still flow towards the cathode.¹ EOF is much greater than electrostatic attraction, and regardless of the charge of the molecule, it will flow in one direction towards the cathode and separate during one run.

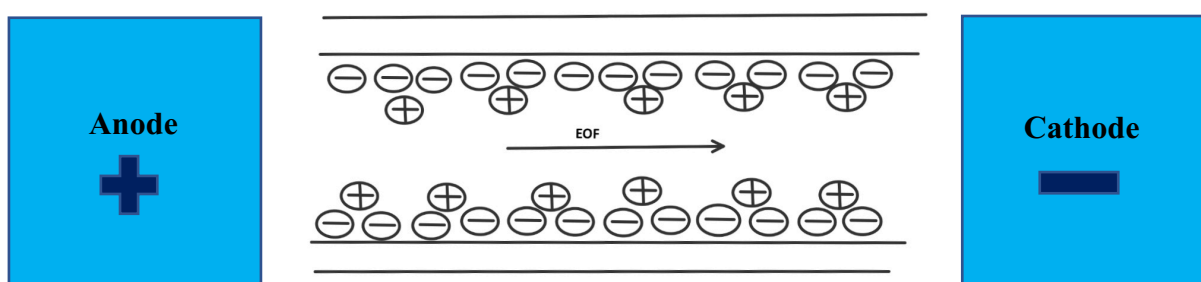


Figure 2. Electroosmotic flow diagram in the capillary showing the charged double layer from the cations in the buffer.

As a result of separation in CE is based on the charge of an ion, the velocity and mobility of an ion can be determined by the following equations:

$$v_{\text{ion}} = \mu_e E \quad (1)$$

$$\mu_e = \frac{q}{6 \cdot \pi \cdot \eta \cdot r} \quad (2)$$

where μ_e is the electrophoretic mobility, E is the strength of the electric field being applied, q is the charge of the ion, η is the viscosity of the buffer solution, and r is the radius of the ion.¹ The variables in this equation depend on the type of ion, as well as the pH of the buffer.¹

There are two factors that affect EOF: the pH of the buffer used and suppression of flow.^{1,6} The pH of the buffer has to be considered regarding EOF, because it can affect the charge separation within the capillary.¹ When the buffer has a high pH, the silanol groups stay deprotonated and charged, allowing for the formation of a strong double layer.^{1,7} When the buffer has a low pH, the silanol groups are protonated and are neutral, resulting in a weaker double layer and weak EOF.^{1,6,7}

Suppression of flow also has an effect on the EOF, because if there is no current flow, the solution is prevented from traveling to the cathode where the products can be detected. This could be due to bubble formation or a blockage in the capillary. Bubble formation occurs when the capillary is not fully submerged in the sample during injection, if the capillary is placed above the electrode during injection, or if the sample in the capillary becomes dislodged when placing back into the inlet buffer solution. Another cause for bubble formation is due to Joule heating. Joule heating occurs when there is too much current flowing, due to increasing the applied electric field or the ionic strength of the buffer.⁸ The temperature increases too much in the center of the capillary, which can result in bubble formation or laminar flow.¹ However, Joule heating can be prevented by thermostating the capillary to keep the temperature stable when current is flowing. A blockage can occur if the capillary was not washed thoroughly. Both bubble formation and a blockage in the capillary can be resolved by washing the capillary with buffer.

An advantage of capillary electrophoresis is that the EOF causes the solution to flow through the capillary with a flat flow profile, or plug flow, which is shown in Figure 3.¹ Since EOF is caused by an electric field and is able to occur because of the charged double layer surrounding the capillary, and results in separation based on the charge of the ion. This will

allow the EOF to be uniform throughout the capillary and results in a flatter shape. The flat flow profile increases the efficiency of separation, and there will be an increase in the number of theoretical plates (N).¹ In systems with laminar flow, the flow has a parabolic shape and will have lower resolution, since it is caused by a frictional force along the walls of the stationary phase and the solution.^{1, 3, 9, 10} Compared to laminar flow that occurs in high performance liquid chromatography (HPLC) because of a high pressure pump, EOF can be more efficient for separation and can have a greater resolution.^{1, 6, 7}

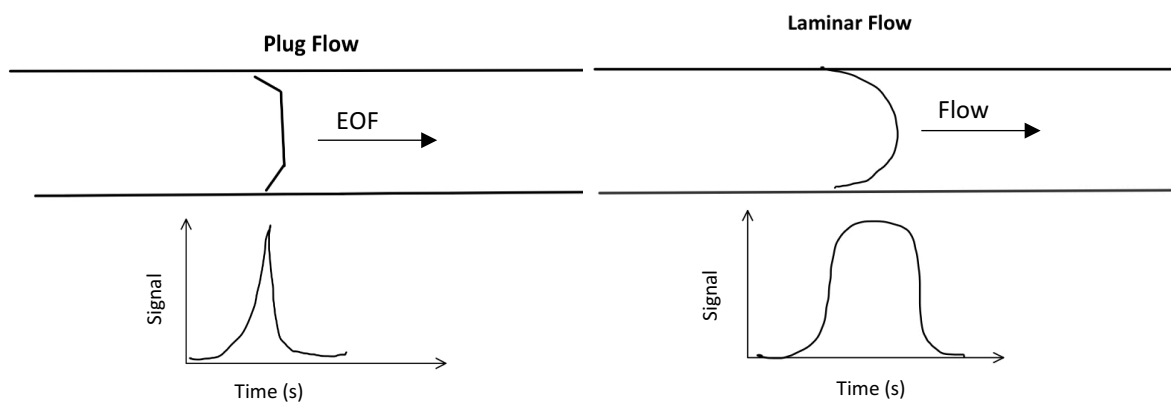


Figure 3. Different types of flow profiles that can occur in a capillary, with the expected responses.¹

Depending on the type of sample being injected into the CE system, there are three types of sample injections that can be performed: hydrodynamic, electrokinetic, and pressure injections.^{1, 3, 11} In hydrodynamic injections, the sample is placed at a higher elevation, and when the capillary is placed in the sample for a few seconds, the height difference allows for the sample to move into the capillary. For electrokinetic injections, both the capillary and the anode are placed in the sample, and when a high voltage is applied for a few seconds, the sample is introduced to the system, and then placed back into the anode reservoir.¹ For pressure injections, pressure is applied in the sample or a vacuum is applied in the cathode reservoir, so when the capillary is placed in the sample, there is enough pressure to move the sample into the capillary.¹

Capillary electrophoresis is often advantageous because of its high efficiency; however, a limitation of this separation method is its detection limits.^{12, 13} Capillary electrophoresis is often paired with optical detection, such as UV-Vis absorption, because it is nearly a universal detector.^{1, 4} UV-Vis absorption does not have good detection limits because of problems with the pathlengths.^{4, 14} This is due to the outer diameter of the capillary being approximately 360 μm , thus making the path length much shorter than the typical one centimeter.¹ Other types of optical detectors paired with CE include laser induced fluorescence, fluorescence, and photodiode arrays (PDAs).^{1, 15} These other methods have better sensitivity than UV-Vis absorption, but due to the fact they are all types of on-column detectors, they will also have higher detection limits because of smaller path lengths.^{1, 4, 6, 15}

Electrochemical detection can be used as an alternative detection method for CE, because of its high sensitivity. These methods can be separated into three categories: potentiometric, conductometric, and amperometric detections.¹⁶⁻¹⁸ Potentiometric detection are ion selective, and are able to detect the ion of interest in small volumes of sample when a potential difference is applied.¹⁷ Conductometric detection utilizes a potential difference between two electrodes in an electrolytic sample.¹⁷ Amperometric detection is highly sensitive and selective, and transfers electrons when a voltage is applied.^{1, 17} Electrochemical detection can be favored because of its sensitivity and selectivity, but this type of detection also has its limitations.¹⁶ One of the main limitations is that it can interfere with the applied voltage, causing fluctuations in the current flowing across the capillary.¹⁶ These electrochemical methods are all post-column detectors, making it problematic to be paired with capillary electrophoresis systems that utilize post-column detection cells. With the cathode is in the outlet cell, and in close proximity to the detector, the increased current leads to noise.^{16, 17} Another limitation of electrochemical detection

CE-CL has also been widely used, because chemiluminescence is a type of detection that does not require an external light source.^{22, 24, 27} Due to chemiluminescence not requiring an external light source, there will be reduced background noise, in addition to high sensitivity and selectivity when paired with CE because it is usually performed in the dark.^{2, 15, 19, 22-24, 26, 27}

However, a significant drawback to using CE-CL is that luminol is sensitive to pH.^{14, 24, 26, 28} If the pH of the buffer used is too high, the intensity of the peak increases. Conversely, if the pH of the buffer is too low, the intensity of the peak will decrease.²⁸ This is due to the conditions for luminol to be oxidized when reacting with hydrogen peroxide to produce light, and depending on the pH, there will either be an increase or decrease in amount of light produced. A possible reason to alter this condition is because another reagent (such as an enzyme) being used in the reaction requires a different pH to react for optimal activity. Another drawback to using CE-CL is that there is a limitation on the reagents that can be used with luminol. This limits the type of enzyme or chemical used because luminol has to react with hydrogen peroxide in order for chemiluminescence to occur. For this project in particular, it was limited to only enzymatic reactions that produce hydrogen peroxide. Glucose oxidase, the model enzyme, produced hydrogen peroxide as a byproduct, which resulted in the reaction with luminol in the outlet cell and produced light.

Electrophoretically mediated microanalysis

Enzyme kinetics have been used to determine the rate of the enzymatic reaction, and a generic enzyme reaction is shown in the equation below:



Equation 3 shows that when an enzyme and substrate react, the substrate binds to the enzyme's active site, creating the enzyme-substrate complex (ES), and product is formed after the substrate

is converted to product at the active site.²⁹ When the enzyme and substrate react to form the enzyme-substrate complex, it can occur in two different ways: under the lock and key model or the induced fit model, which are shown in Figure 5.

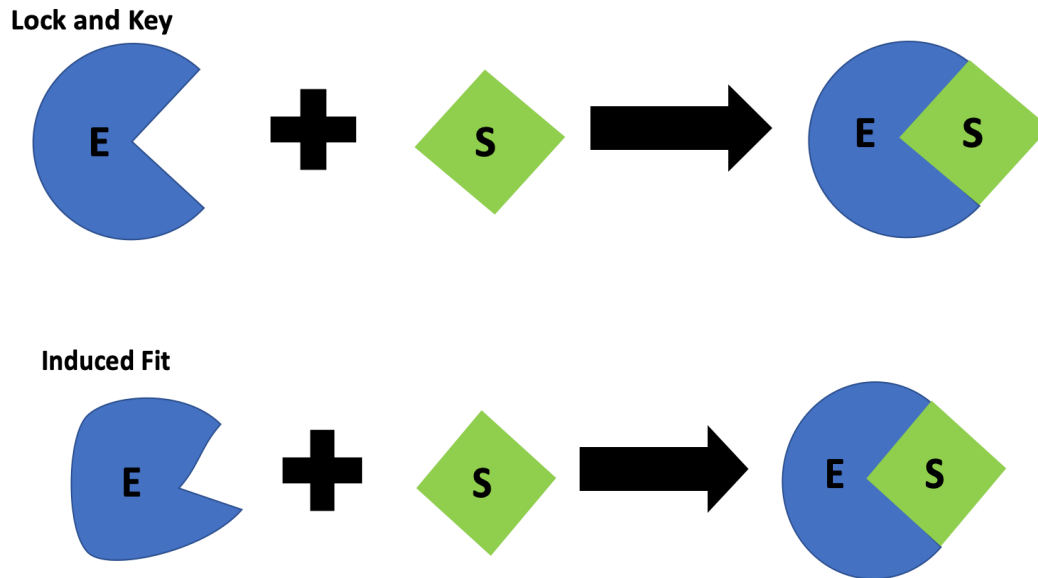


Figure 5. Lock and key model (A) and the induced fit model (B) for ES complex binding.³⁰

For the lock and key model, the shape of the substrate is complementary to the shape of enzyme's active site, and is able to bind to form the ES complex with no conformational change. For the induced fit model, the enzyme's active site has to undergo a conformational change in order for the substrate to be able to fit and form the ES complex. The steps in this reaction are important in determining the Michael-Menten constant of the enzyme of interest. The Michaelis-Menten equation is:

$$v_o = \frac{V_{max}[S]}{K_m + [S]} \quad (4)$$

where V_{max} is the maximum velocity (or rate) of the enzyme, $[S]$ is the substrate concentration, and K_m is the Michaelis-Menten constant of a particular enzyme.²⁹ This equation is useful for

seeing how the rate changes in response to varying the substrate concentration when the enzyme concentration is held constant. The K_m value can be determined on the Michaelis-Menten plot as the substrate concentration at half V_{max} and be compared to literature values, which is shown in Figure 6A. Another way for the K_m value to be determined by linearizing the Michaelis-Menten graph using a Lineweaver-Burk plot. The Lineweaver-Burk plot equation resembles a line of best fit, which is:

$$\frac{1}{v_o} = \left(\frac{K_m}{V_{max}} \right) \frac{1}{[S]} + \frac{1}{V_{max}} \quad (5).$$

By taking the inverse of the Michaelis-Menten plot, the K_m can be determined by setting the negative inverse of the K_m equal to the x-intercept of the line, which is shown in Figure 6B. The K_m value indicates the type of binding that occurs at the ES complex. A lower K_m value indicates that tight binding is occurring and there is more ES complex forming so there will also be more product formation. A higher K_m value indicates that weak binding is occurring and there is more ES complex dissociating than forming, therefore less product.

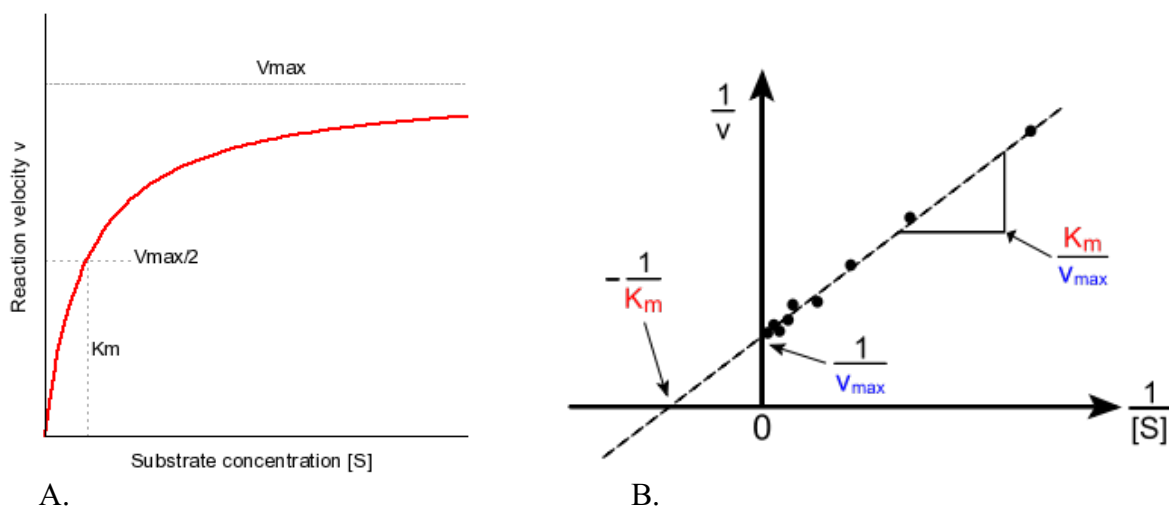


Figure 6. Example Michaelis-Menten plot (A) and Lineweaver-Burk plot (B).^{31, 32}

Electrophoretically mediated microanalysis (EMMA) is used to continuously mix and separate the enzyme, substrate, and products.³³⁻³⁵ This is achieved by injecting a plug of enzyme into the capillary containing substrate, which is shown in Figure 7. In order to construct a Michaelis-Menten or Lineweaver-Burk plot to determine the rate of the enzymatic reaction, the enzymatic rates can be determined from obtaining plateaus of the reaction using EMMA.

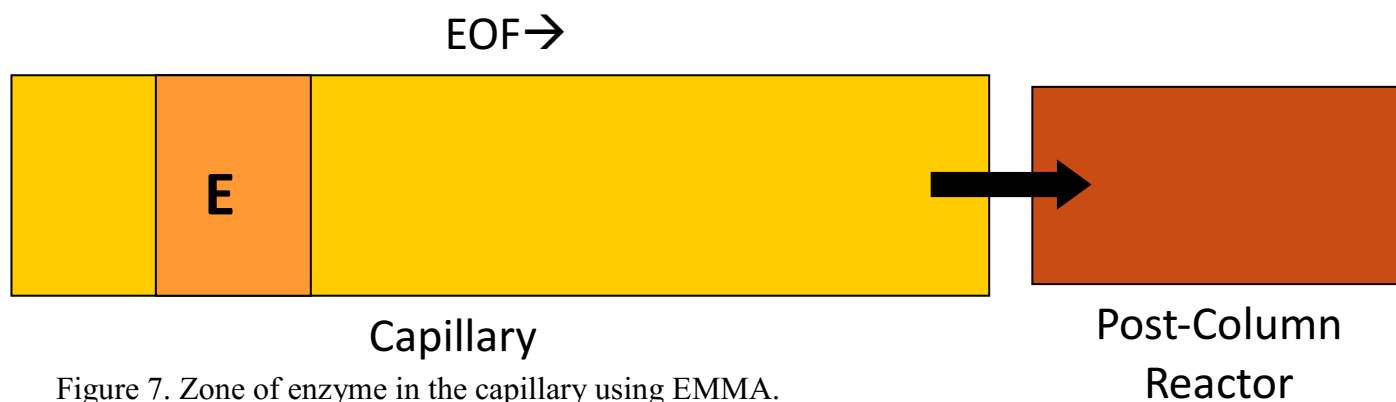


Figure 7. Zone of enzyme in the capillary using EMMA.

When the zone of enzyme is injected into the system, EMMA can be used under either zero potential or constant potential.^{29, 36, 37} Under zero potential, there is no current flow, so there would be no EOF to separate the enzyme and substrate.²⁹ This is done to leave the enzyme and substrate to mix without separation, and product would form.^{29, 37} Under constant potential, the enzyme and substrate are constantly mixed, product formed, and separated from each other as they progress through the capillary.²⁹

When EMMA is performed under constant potential, there are three types of responses that can occur during the reaction. The first type of response that can occur is when the enzyme, substrate, and product are all mixing and separating continuously that the reaction detected will show a constant EMMA plateau, which is shown in Figure 8A. The second type of response involves the product being formed, or having excess product from the previous trial, before the

enzyme was introduced into the system by electrokinetic injection.²⁹ When this occurs, the product will be detected first and have a higher response on the EMMA plateau, which is shown in Figure 8B. The final type of response involves excess product being detected at the end.²⁹ When this occurs, the product has more time to mix and separate in the capillary, so the response will be much greater on the EMMA plateau, which is shown in Figure 8C.

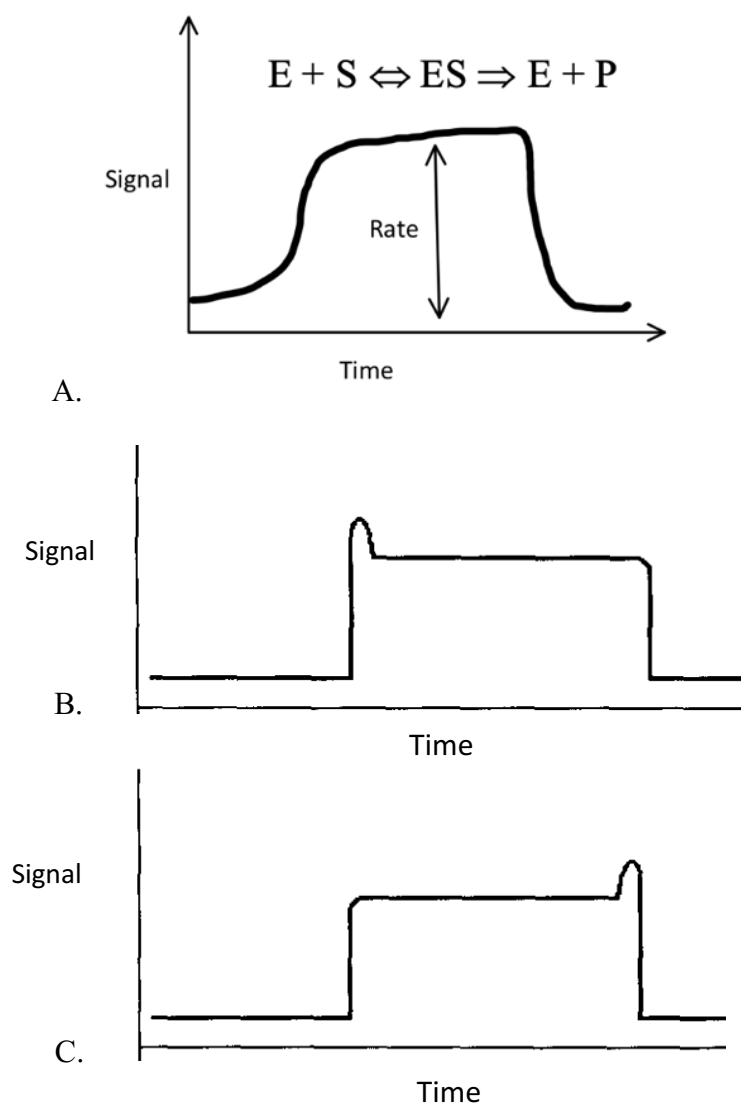


Figure 8. Example of expected EMMA plateau (A), EMMA plateau where excess product is detected first (B), and EMMA plateau where excess product is detected at the end (C).²⁹

their electrophoretic mobilities.³³ The inhibitor zone has to be injected during the formation of the ES complex, so they can mix and separate, which results in a dip on the EMMA plateau because of a decrease in product formation.³³ The work done by Whisnant and Gilman was an effective method for demonstrating that the presence of an inhibitor in the capillary electrophoresis system can be used to measure inhibition constants.

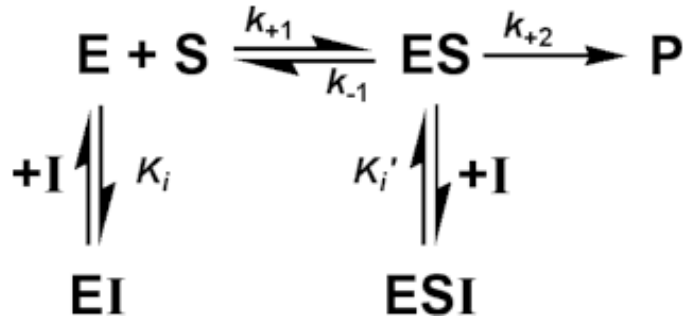


Figure 10. Enzyme inhibition reaction.

The three types of inhibitors are competitive, uncompetitive, and non-competitive. A competitive inhibitor binds at the enzyme's active site, because it has a structure that is similar to that of the substrate, and ultimately prevents the formation of the ES complex.³³ This type of inhibitor does not affect the V_{\max} value of the enzyme but does increase the K_m value, which is shown on the Lineweaver-Burke plot in Figure 11A, where both plots have the same y-intercept.

Noncompetitive inhibitors bind either to enzyme or the formed ES complex.³³ This type of inhibitor only affects the V_{\max} of the enzyme. As the concentration of the inhibitor increases, there is a decrease in V_{\max} but the K_m value remains the same, which is shown on the Lineweaver-Burke plot in Figure 11B, where both plots have intersecting x-intercepts.

Uncompetitive inhibitors bind to the formed ES complex, and decreases the amount of product formed.³³ This type of inhibitor affects both the V_{\max} and K_m of the enzyme. As the concentration

of the inhibitor increases, there is a decrease in both the K_m and V_{max} , which is shown on the Lineweaver-Burke plot in Figure 11C, where the plot has non-intersecting lines.

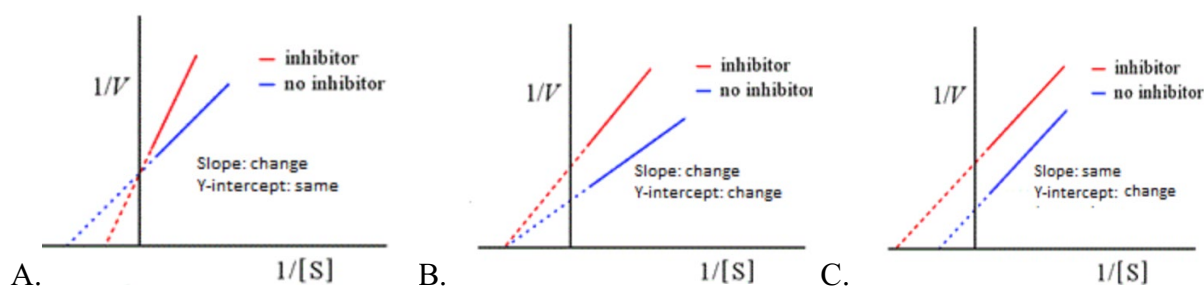


Figure 11. Lineweaver-Burk plots of competitive inhibition (A), noncompetitive inhibition (B), and uncompetitive inhibition (C).⁴⁰

For this project, a known, competitive inhibitor of glucose oxidase that can be used as a is chloride.³⁹ At low pH, chloride ions are a competitive inhibitor for glucose oxidase, and will bind to the active site of the oxidized form of the enzyme.^{39, 41, 42} However, the conditions for this project uses a buffer with pH = 10.80, and does not satisfy these conditions for chloride ions. Another type of inhibitor that can be used is 2-deoxy-D-glucose, which is shown in Figure 12.³⁹ This is a competitive inhibitor, because it has a similar structure to the substrate, and is able to bind to the enzyme's active site.³⁹

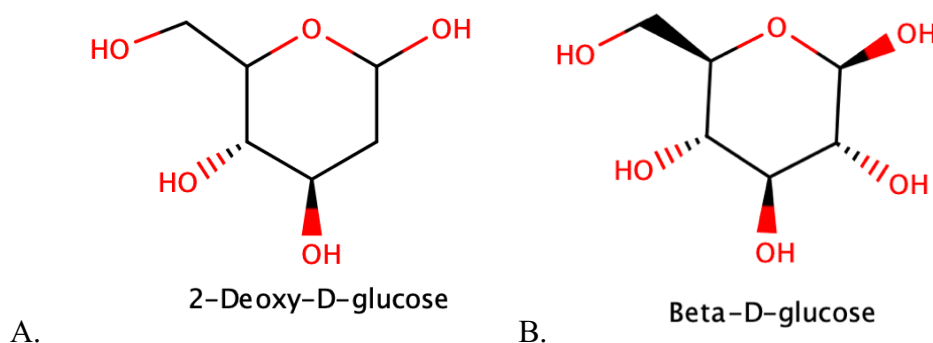


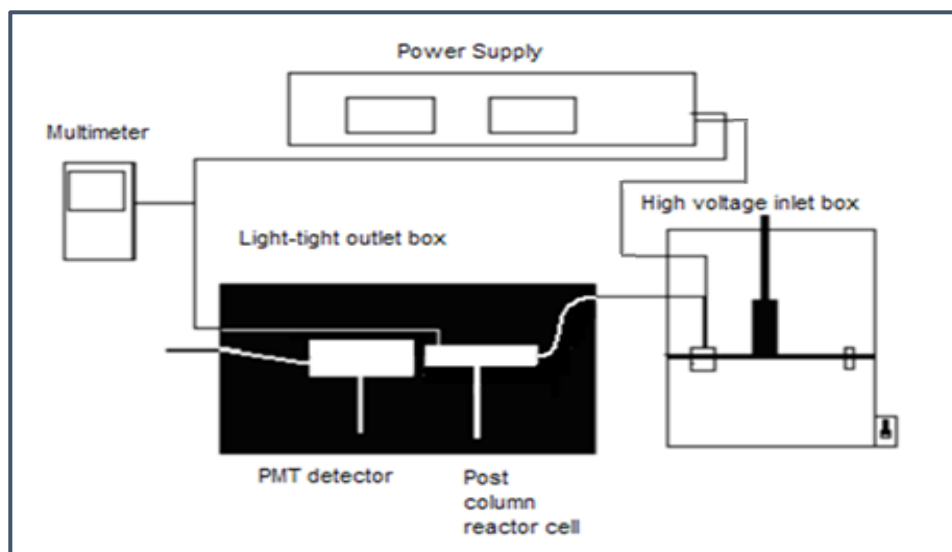
Figure 12. Structure of competitive inhibitor (A) and substrate (B).

Materials and Methods:*Reagents*

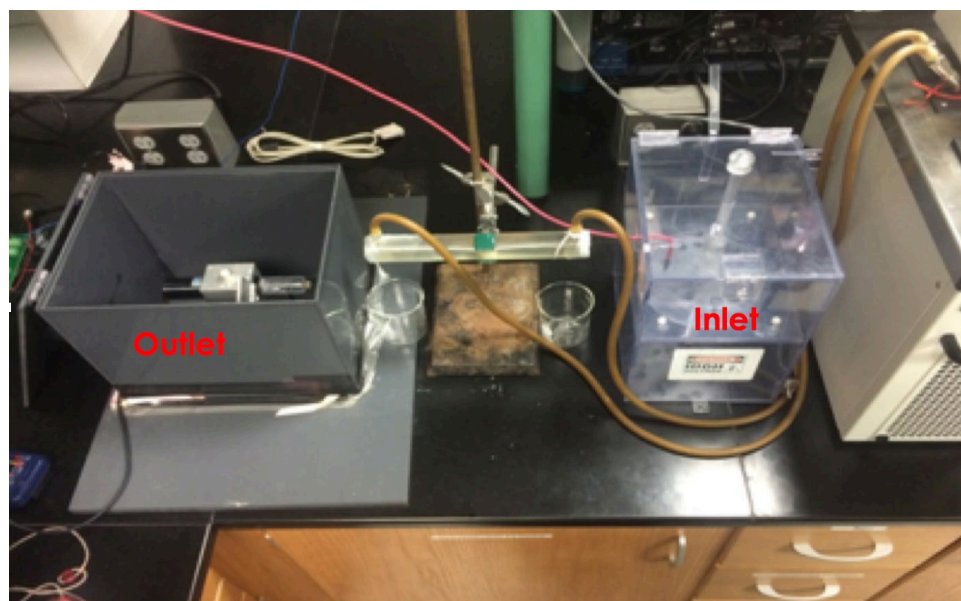
Microperoxidase (CAS 104870-94-2) and luminol (CAS 521-31-3), glucose oxidase (CAS 9001-37-0, 10 kU), methanol (CAS 67-56-1) and hydrogen peroxide (CAS 7722-84-1, 30% w/w) were purchased from Sigma Aldrich. β -D-glucose (97%, CAS 492-61-5) was purchased from MP Biomedicals. Sodium phosphate tribasic (CAS 10101-89) and sodium phosphate dibasic (CAS 7558-79-4) were purchased from Fisher Scientific, which were combined to make the sodium phosphate buffer used (pH =10.80, 1.3780 g Na_2PO_4 , 0.1114 g Na_3PO_4).

The instrument

For both the luminol and glucose oxidase injections, a custom CE-CL system was used, which are shown in Figures 13A and 13B. In the outlet box, the post-column detector (which is the photon counter) is connected to the computer monitor through a National Instrument data acquisition board (CB-68LP) in which a photon counter program is utilized in LabVIEW, as shown in Figure 14. A Spellman power supply (CZE1000R) was used to apply a constant potential of 15 kV and allow current to flow across the capillary during each run, and the capillary used was purchased from Polymicro Technologies (363 μm outer diameter, 75 μm inner diameter).

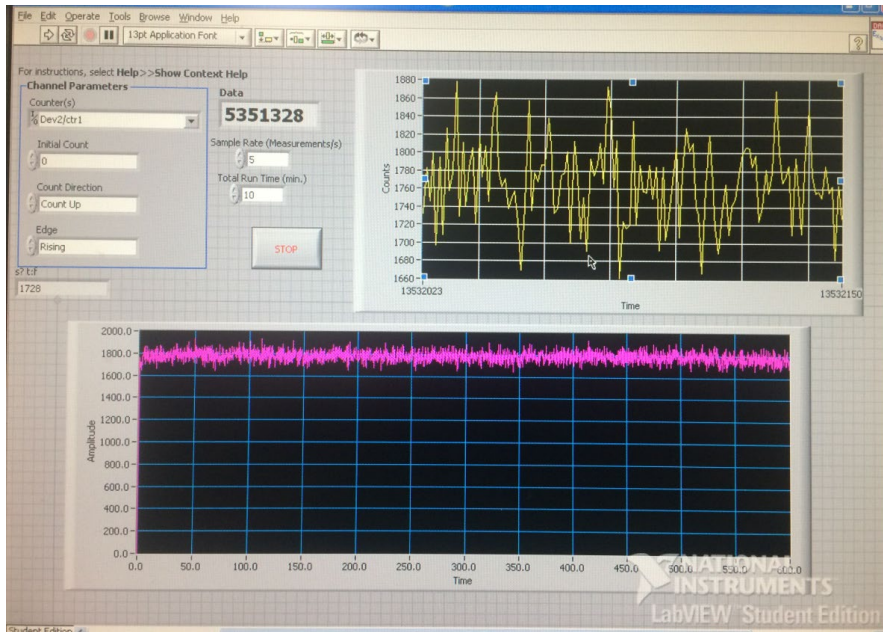


A.

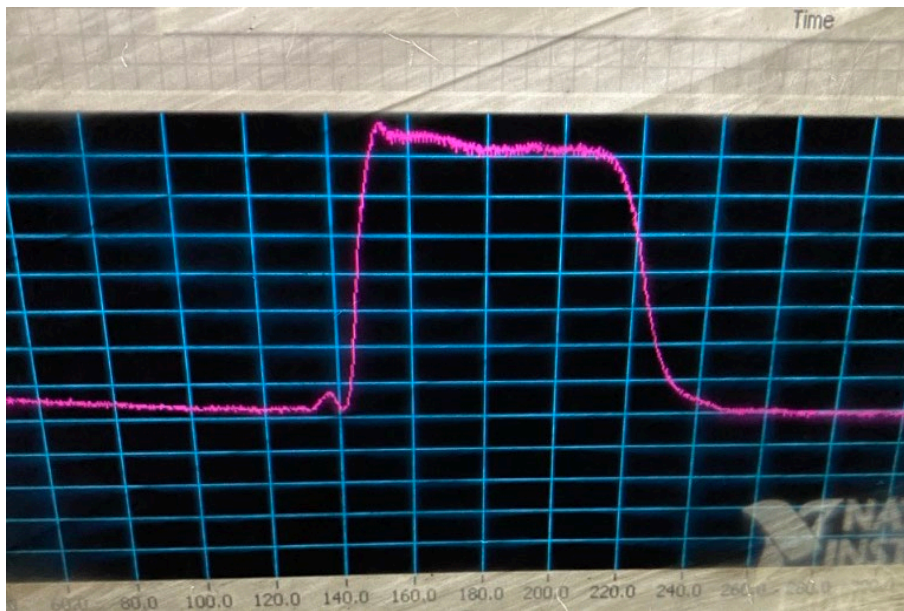


B.

Figure 13. Diagram of the CE-CL system (A) and custom CE system with post-column chemiluminescence detection (B).



A.



B.

Figure 14. Photon counter program used on LabVIEW (A) and EMMA plateau (B).

Preparing the capillary

Before the first run, or whenever suppression of flow occurred, the capillary had to be washed in this order with: 0.1 M sodium hydroxide, DI water, then with sodium phosphate buffer. In order to do this, a custom capillary adapter was used and attached to a syringe.

Validation of the instrument: luminol injections

For the validation of the instrument, various concentrations of luminol were used to measure the consistency of the trials performed. A 1.0 mM luminol stock solution was prepared by weighing 0.0089 g and quantitatively transferring it to a 50.00 mL volumetric flask with 5.00 mL of methanol. The solution was sonicated until the luminol fully dissolved, and was then diluted to the mark with sodium phosphate buffer. A 0.215 mM microperoxidase stock solution was prepared by weighing 0.0042 g and quantitatively transferring it to a 10.00 mL volumetric flask to be diluted to the mark with sodium phosphate buffer. A 0.4 M hydrogen peroxide stock solution was prepared by weighing out 0.435 g in a 10.00 mL volumetric flask and diluting to the mark with sodium phosphate buffer.

The capillary (37.0 cm) was placed in the inlet and outlet cells. In the inlet, the anode and capillary were placed in a beaker filled with 0.215 mM microperoxidase solution, while the cathode and capillary in the outlet cell were placed in 0.4 M hydrogen peroxide. The luminol sample was prepared in an Eppendorf tube and diluted with sodium phosphate buffer. This Eppendorf tube was taped above the anode on the inlet box. The capillary was then placed in this sample to allow the luminol to be introduced into the system by a five second hydrodynamic injection, then placing it back into the microperoxidase solution. The parameters set for the luminol injections on the Photon Counter LabVIEW program were a 6-minute runtime, with 5 measurements/second.

Glucose oxidase injections

For the glucose oxidase injections, various concentrations of the enzyme were used to determine the optimal concentration for this portion of the project. The luminol and microperoxidase stock solutions were prepared the same way as the luminol injections. A 2.50×10^{-5} M microperoxidase/ 2.50×10^{-6} M luminol solution was prepared by adding 1.00 mL of the microperoxidase and 75.0 μ L of luminol stock solutions in a 10.00 mL volumetric flask, and diluting to the mark with sodium phosphate buffer. A 200.0 mM β -D-glucose stock solution was prepared by weighing out 3.60 g and quantitatively transferring it to a 100.0 mL volumetric flask to be diluted to the mark with sodium phosphate buffer. A glucose oxidase stock solution was prepared by adding 200.0 μ L to a 10.00 mL volumetric flask and diluting to the mark with sodium phosphate buffer.

Once the optimal glucose oxidase concentration was determined, the concentration of the substrate, β -D-glucose, was varied. Using the 200.0 mM β -D-glucose stock solution, a series of 10.00 mL dilutions were performed to vary the concentration between 5.00 mM-100.0 mM.

In the inlet, the anode and capillary were placed in a beaker filled with 200.0 mM β -D-glucose stock solution, while the cathode and capillary in the outlet cell were placed in the 2.50×10^{-5} M microperoxidase/ 2.50×10^{-6} M luminol solution. Before the run could begin, the β -D-glucose solution had to flow through the capillary. The glucose oxidase sample was prepared in an Eppendorf tube and diluted with sodium phosphate buffer, and the Eppendorf tube was placed in the inlet box. The capillary and anode were then placed in this sample to allow the glucose oxidase to be introduced into the system, by a five second electrokinetic injection, then placing both back into the β -D-glucose solution. The parameters set for the glucose oxidase injections on the Photon Counter LabVIEW program were a 6-minute runtime, with 5 measurements/second.

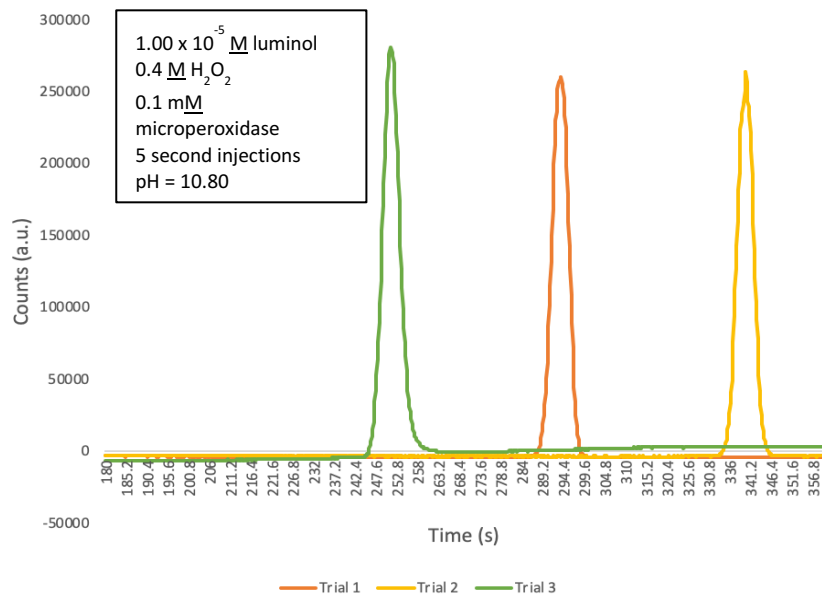
Results and Discussion:

Validation of the instrument: luminol injections

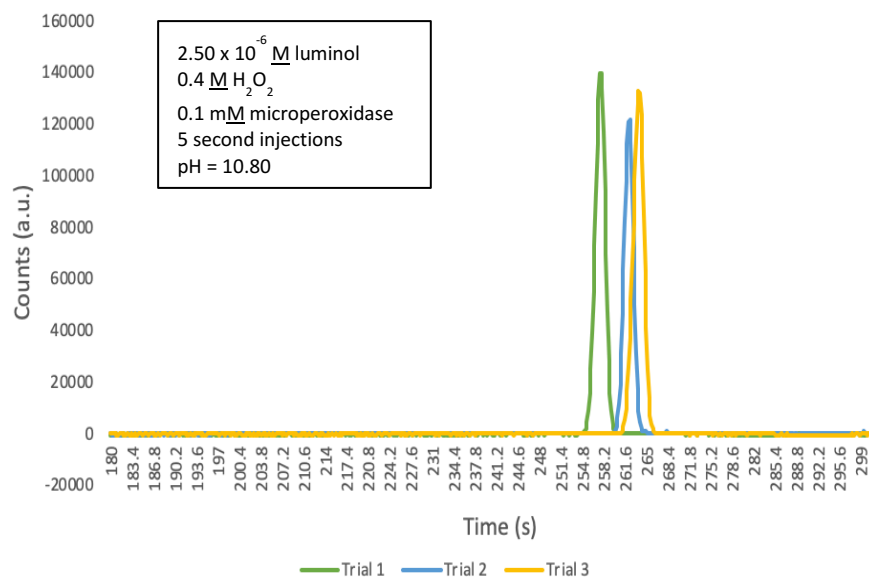
Validation of the instrument was performed in order to learn how to use the custom CE-CL system, as well as obtaining consistent responses using different concentrations of luminol. During this method, luminol is injected into the capillary and reacts with hydrogen peroxide in the outlet cell to produce light, in which the signal detected by the photon counter would be a peak. In order to learn how to use the system and obtain consistent results, replicates using multiple concentrations of luminol had to be obtained, as shown in Figure 15. Due to the fact that CE-CL system used is not automated, the retention times of the peak will not always be the same because of the time it takes to have the system in order before the trial starts. However, the intensity of the peak is what should be consistent throughout the trials. It is also expected that as the concentration of luminol increased, the peaks increased, which is shown in Figure 16.

The results from the validation of luminol injections confirmed that the response to the reaction occurring significantly increases when using increasing concentrations of luminol, which is shown in Figure 17A. Using the maxima of the peaks obtained from increasing luminol concentrations, a calibration curve was created to determine if there was consistency in the results with the method used, which is shown in Figure 17B. The line of best fit was determined to be $3.0 \times 10^{10}x - 6.7 \times 10^4$, with an R^2 value of 0.9925. The R^2 value indicates that that was strong linearity present as the concentrations of luminol increased.

The luminol injections validated the method and proved to be a reliable and effective method in detecting chemiluminescence. It also showed that there was confidence in the obtained results, and could move forward with the glucose oxidase injections.



A.



B.

Figure 15. Normalization of triplicate luminol injections using 1.00 x 10⁻⁵ M (A) and 2.50 x 10⁻⁶ M (B).

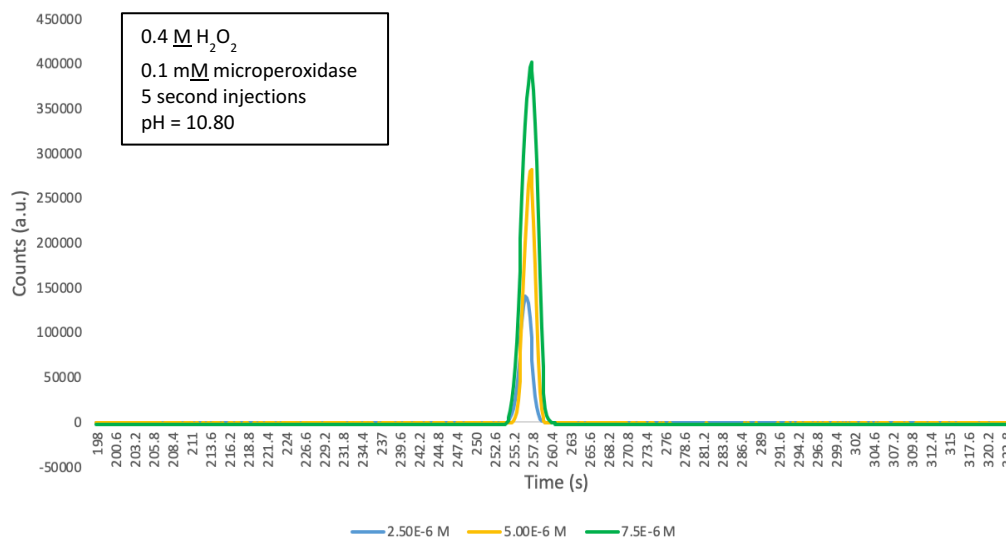
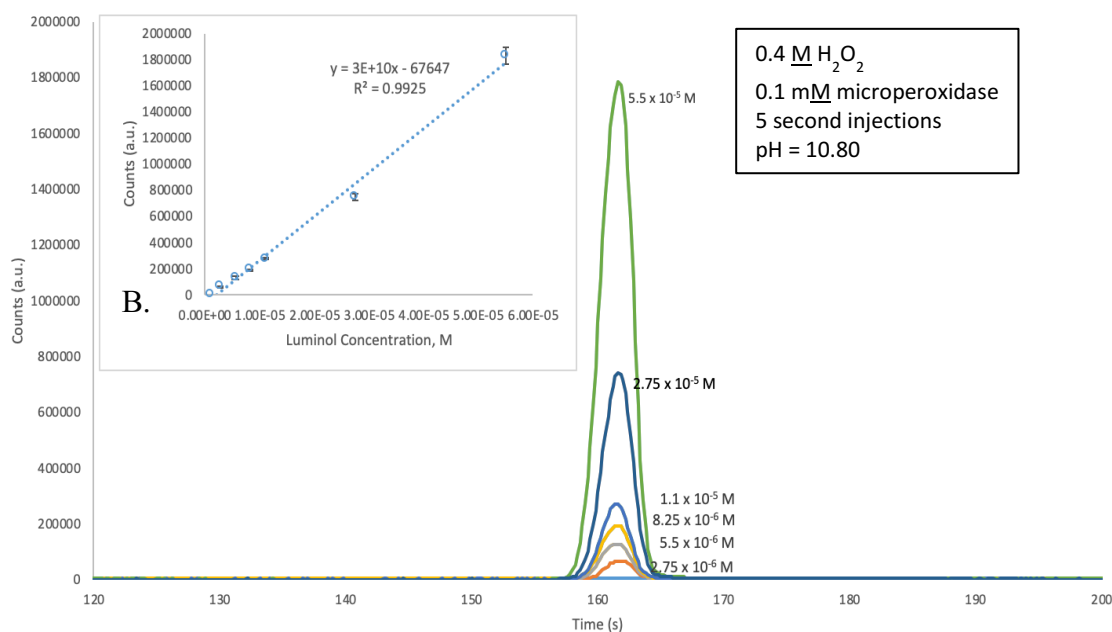


Figure 16. Normalization of various luminol concentrations.

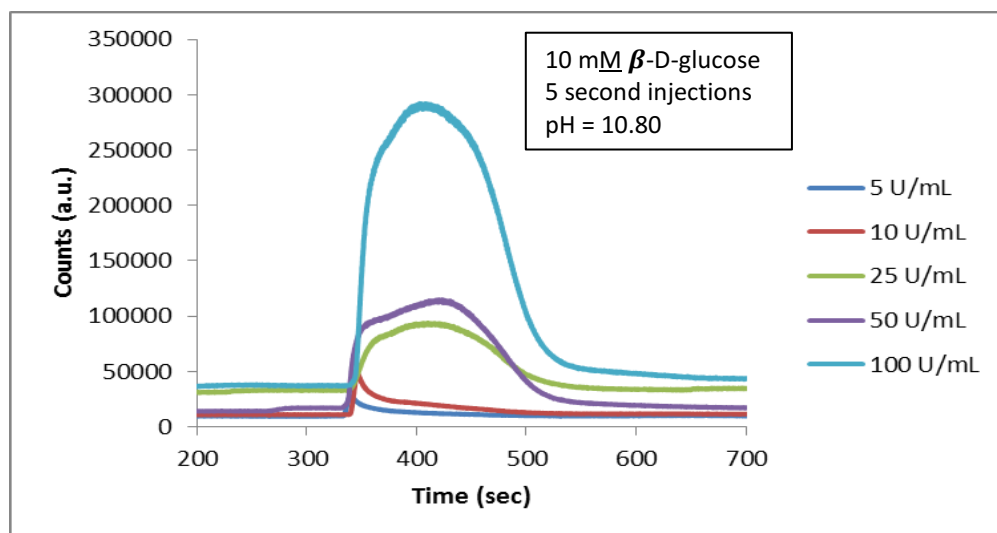


A.

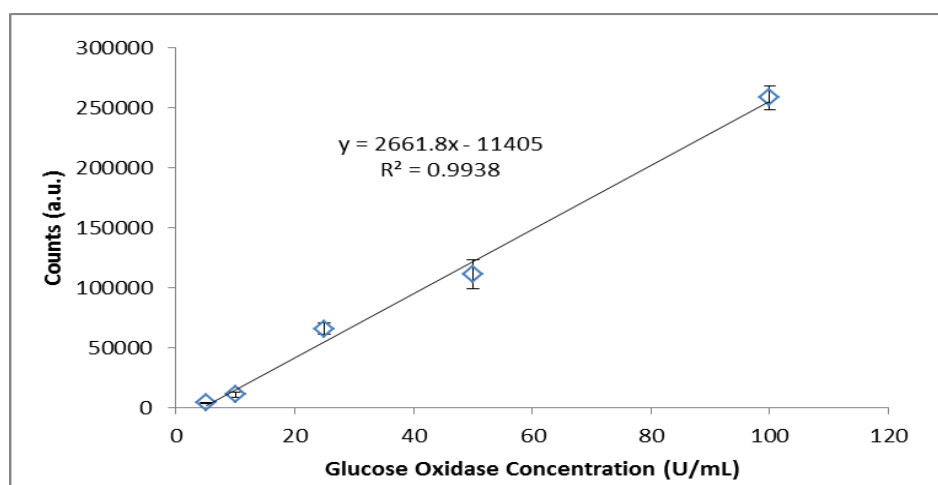
Figure 17. Normalization of various luminol concentrations used (A) and calibration curve (B).

Glucose oxidase injections

The custom CE-CL system was used with EMMA to introduce various concentrations of glucose oxidase by electrokinetic injection to see if a signal was detected by the photon counter, when the byproduct, hydrogen peroxide, reacted with the luminol in the outlet cell. Previous work done by former chemistry major, Blake Seaton, is shown in Figures 18A and 18B.⁴³ As the concentration of glucose oxidase increases, the intensity of the plateau also increases which is supported by the R^2 value of 0.9938, indicating strong linearity present. However, one difference between Blake's results and the ones obtained here is the concentration of the substrate, β -D-glucose, used. In these results, the substrate concentration was held constant at 200 mM, because it was to ensure that there was excess substrate during the enzymatic reaction. Blake's results utilized a constant substrate concentration of 10.00 mM, but the results show that there was not enough β -D-glucose to react with glucose oxidase and have product formation, showing that the results were obtained under non-optimal conditions. Due to this, more results needed to be obtained, as well as more reproducible data for publication. Blake Seaton also proceeded to determine the K_m value of glucose oxidase, which was 24.8 mM, by producing a Michaelis-Menten plot, and linearizing it by a Lineweaver-Burk plot, which are shown in Figures 19 and 20. The K_m value Blake obtained showed that a higher concentration of β -D-glucose was needed for this enzymatic reaction.



A.



B.

Figure 18. Previous results of EMMA plateaus using various glucose oxidase concentrations (A) and the calibration curve (B) (adapted from Blake Seaton).⁴³

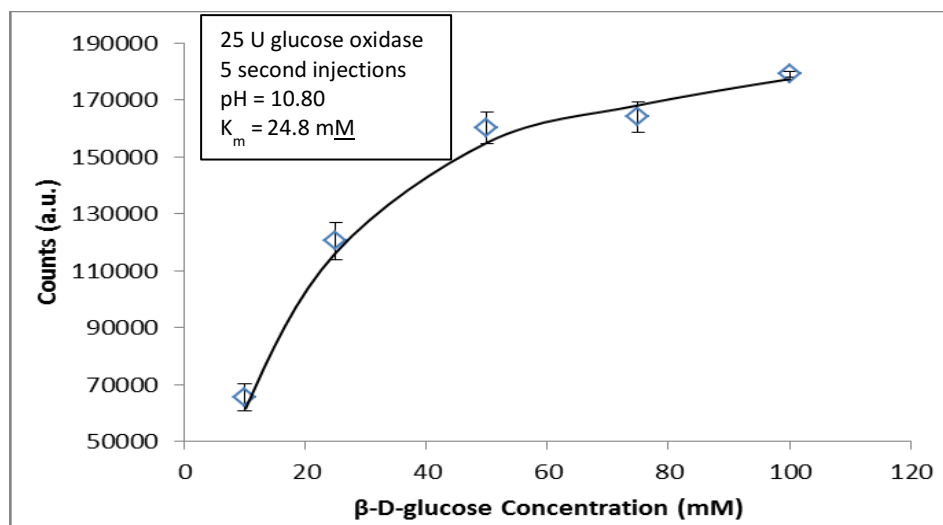


Figure 19. Previous results of a Michaelis-Menten plot of glucose oxidase (adapted from Blake Seaton).⁴³

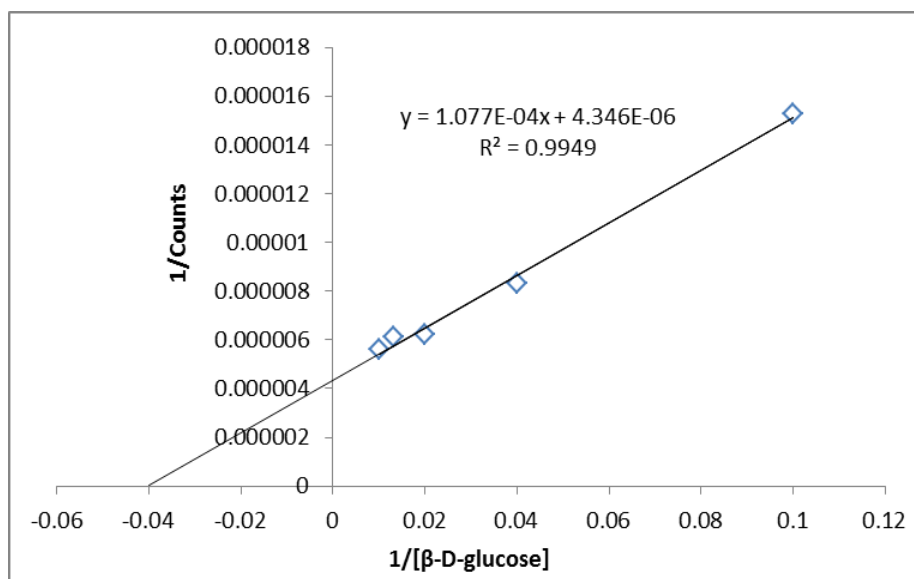
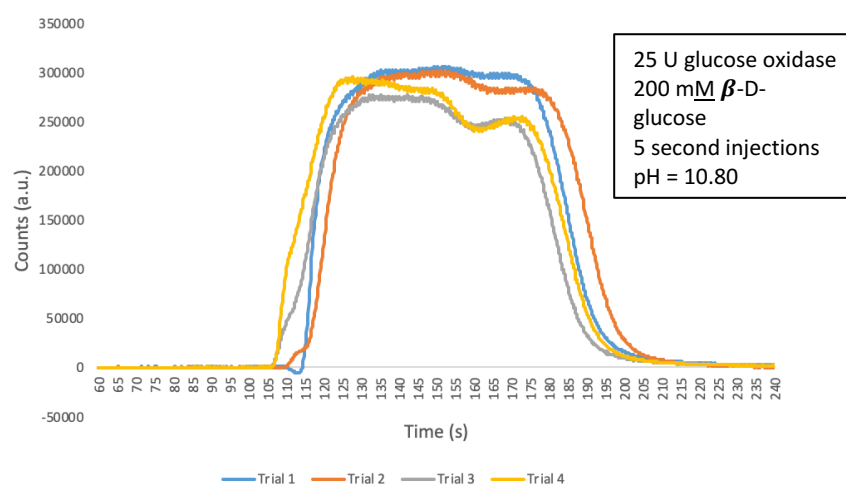
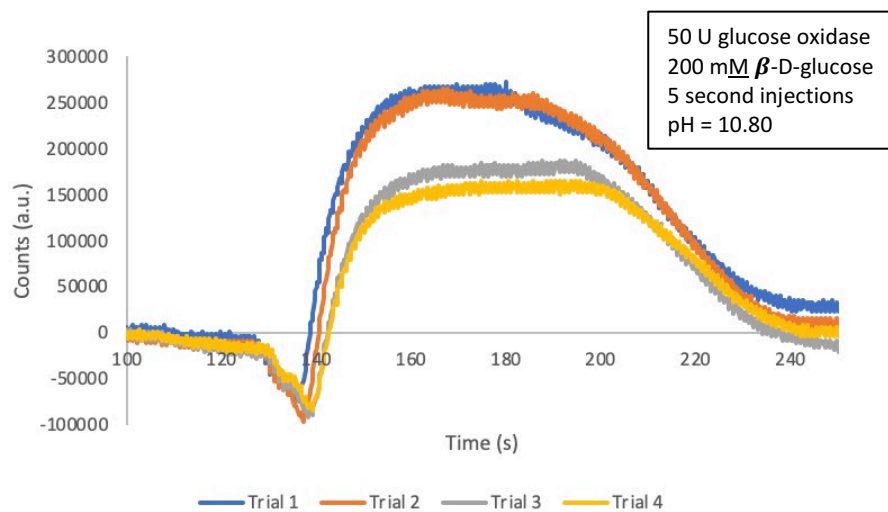


Figure 20. Previous results of a Lineweaver-Burk plot of glucose oxidase (adapted from Blake Seaton).⁴³

As stated in the luminol injection results, this CE-CL system is not automated, so the retention times of the EMMA plateaus will not always be exact throughout multiple trials, but the intensity of the plateaus should be consistent when using the same concentration of glucose oxidase, as shown in Figure 21. Figure 21 also shows that there was consistency between trials and as the concentration of enzyme increased, the rate of the reaction would also increase as a result of a product formation from a high turnover number.



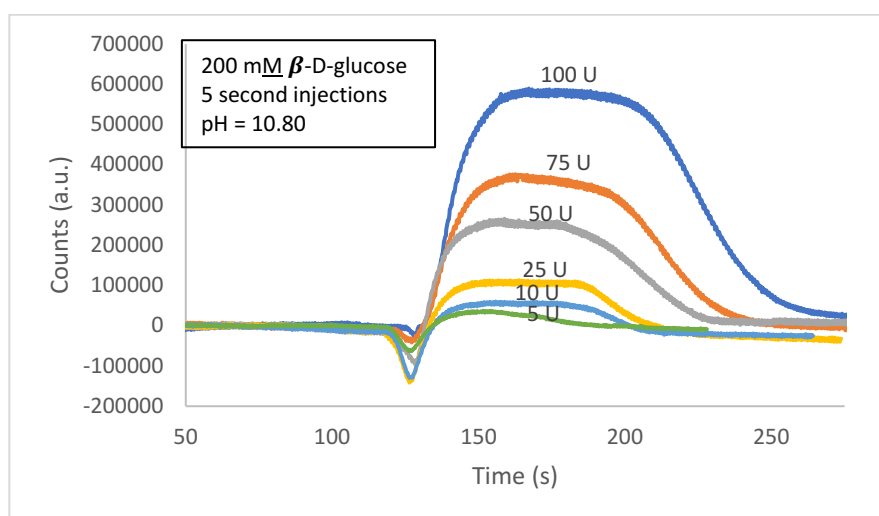
A.



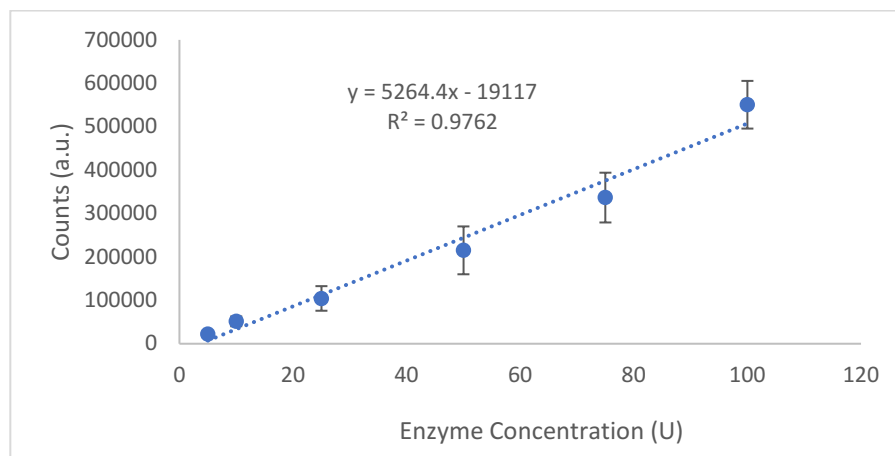
B.

Figure 21. Normalization of replicate trials using 25 U glucose oxidase (A) and 50 U glucose oxidase (B).

The results of the glucose oxidase injections displayed that the response to the formation of product increases when using increasing concentrations of glucose oxidase, which is shown in Figure 22A. Using the average of the constant portion of the EMMA plateaus obtained from increasing glucose oxidase concentrations, a calibration curve was created to determine if the results were consistent throughout the trials performed, which is shown in Figure 22B. The line of best fit was determined to be $5.3 \times 10^3x - 1.9 \times 10^4$, with an R^2 value of 0.976. The R^2 value indicates that that was fairly strong linearity present as the concentrations of glucose oxidase increased.



A.



B.

Figure 22. Normalization of EMMA plateaus using various concentrations of glucose oxidase (U) (A) and calibration curve (B).

One trial was completed to begin the determination of the K_m value of glucose oxidase by constructing a Michaelis-Menten plot and linearizing it by the Lineweaver Burk Plot, which is shown in Figures 23 and 24. This portion of the project will be continue in future work.

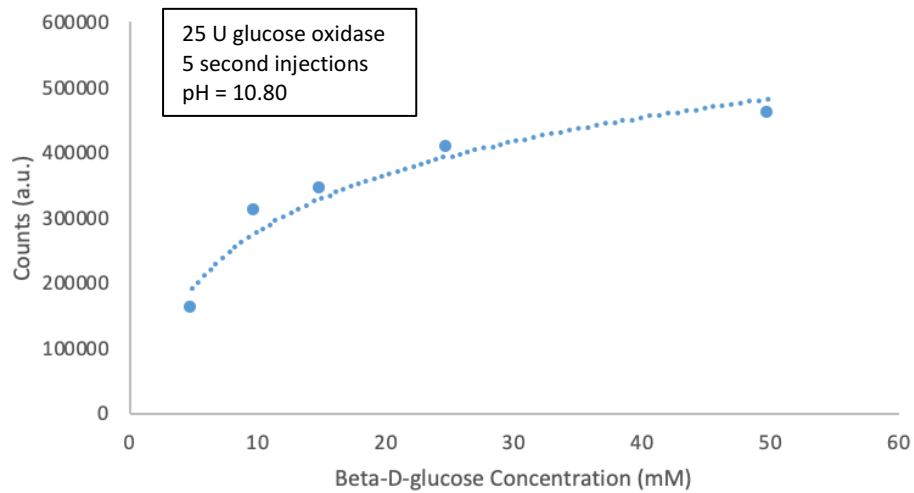


Figure 23. Michaelis-Menten plot of glucose oxidase.

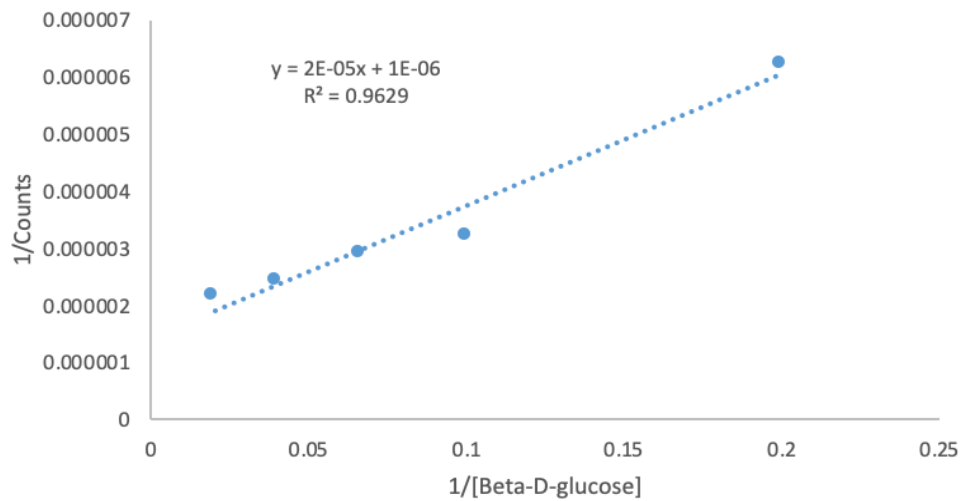


Figure 24. Lineweaver-Burk plot of glucose oxidase.

The results shown in Figures 22-24 were intended to continue for consistency, as well as to complete the data analysis for publication. However, a flood occurred in the laboratory, which caused significant damage to the system and the lab itself. After about three months, experimentation was able to proceed. During trials, there was often no response because the enzymatic reaction was not occurring, having a low signal, significant current drop during trials, or no current flowing through the capillary during trials. Troubleshooting was necessary in order to find the cause of these problems. This process first included replacing the capillary, in case it cracked or was causing flow suppression and checking all reagents used to see which one could be causing this error. Luminol injections were also performed to see if a response would be detected, or if it was a system issue. A peak was observed, but the signal was much lower than expected with the concentration used, indicating that less luminol was being pushed towards the detector after each trial, which is shown in Figure 25. After changing these two conditions with no improvement, all of the solutions were re-made, including the use of DI water from another lab for the buffer. Re-making the solutions had a slight effect on obtaining a response, but the capillary either had a significant current drop or could not hold a steady current, meaning that very little from the inlet was being moved to the outlet cell. It was then determined that the cause of this was not due to anything chemical, but rather a bad cathode, which the results obtained are shown in Figure 26. After replacing the cathode, the system began to function properly, and less noise was observed with the consistent trials, as shown in Figure 27.

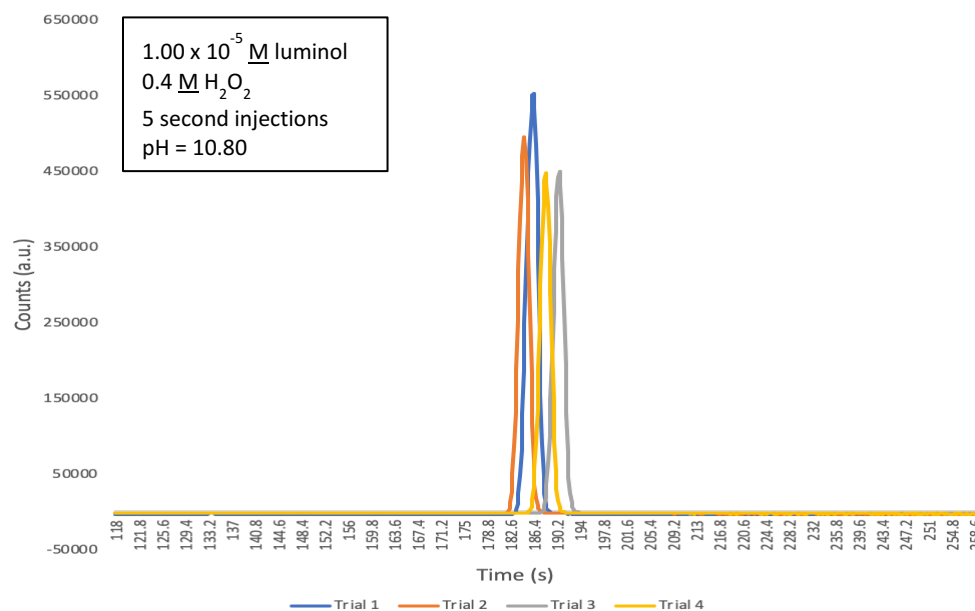


Figure 25. Normalization of luminol injections using 1.00 x 10⁻⁵ M (before changing the cathode).

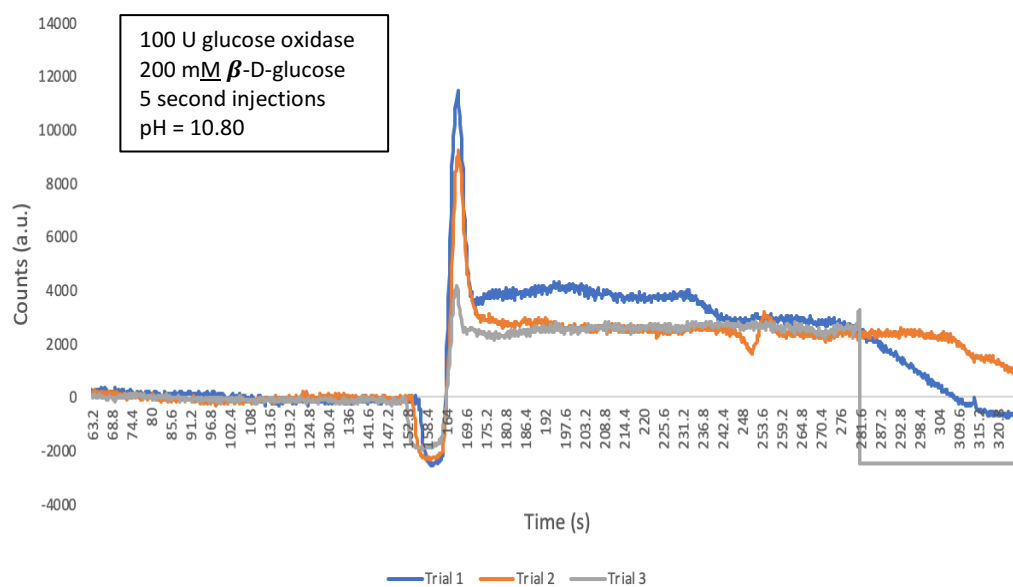
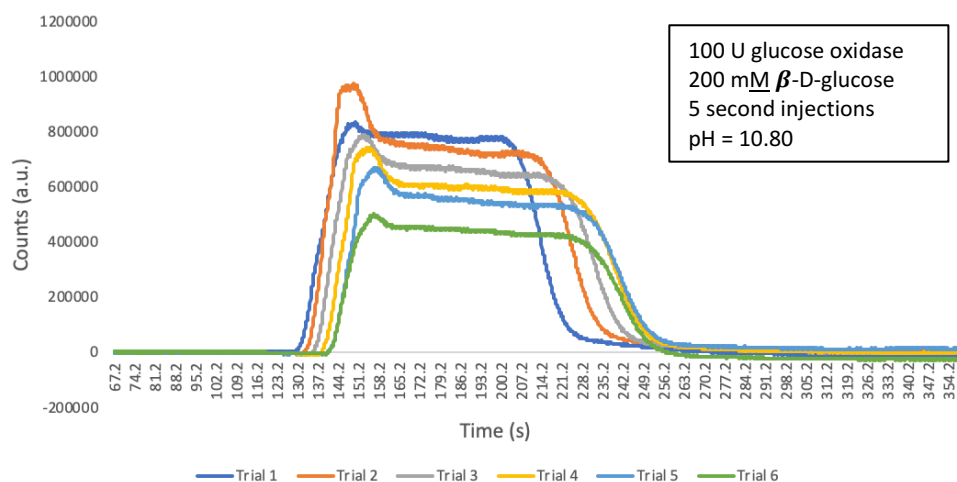
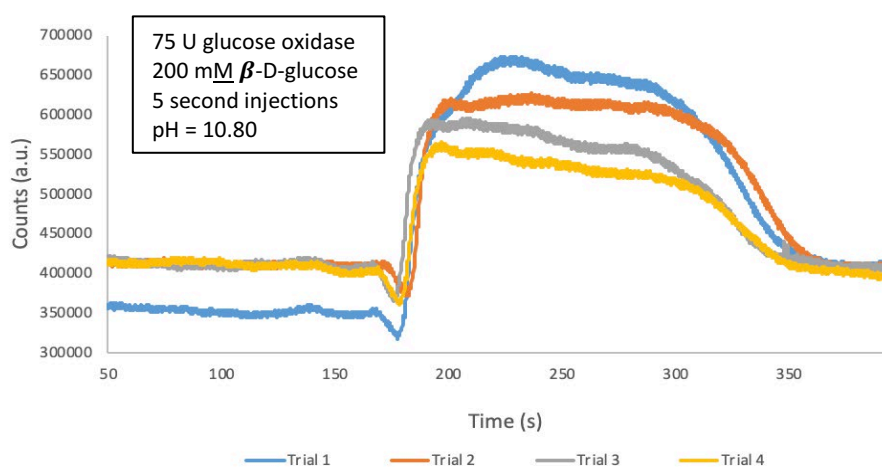


Figure 26. Normalization of EMMA plateaus using 100 U glucose oxidase (before changing the cathode).



A.



B.

Figure 27. Normalization of EMMA plateaus using 100 U glucose oxidase (A) and 75 U glucose oxidase (B) (after replacing cathode).

Conclusion and Future Work:

This research project included validating the instrument and proceeding to the glucose oxidase injections to study the enzyme kinetics of glucose oxidase. After validation, the method of using custom CE-CL system with EMMA to indirectly determine enzyme kinetics has been proven to be very effective and consistent. Future work for this project includes the completion of the data analysis of the glucose oxidase injections to determine the Michaelis-Menten constant, K_m , and compare to the literature values. Future work also includes other inhibitors, such as Co^{2+} , Cu^{2+} , Ag^+ , Mg^{2+} , or 2-deoxy-D-glucose, a competitive inhibitor.³⁹

References:

1. Heiger, D., *High Performance Capillary Electrophoresis: An Introduction*. Agilent Technologies: 2000.
2. Liu, Y.-M.; Cheng, J.-K., Ultrasensitive chemiluminescence detection in capillary electrophoresis. *Journal of Chromatography* **2002**, *959* (1-2), 1-13.
3. Chien, R.-L.; Burgi, D. S., Field amplified sample injection in high- performance capillary electrophoresis. *Journal of Chromatography* **1991**, *559*, 141-152.
4. Dumke, J. C.; Nussbaum, M. A., Adaptation of a Commercial Capillary Electrophoresis Instrument for Chemiluminescence Detection. *Journal of Analytical Chemistry* **2007**, *79* (3), 1262-1265.
5. ChemLibreTexts, Schematic diagram of the basic instrumentation for capillary electrophoresis. The sample and the source reservoir are switched when making injections. 2019.
6. Quirino, J. P.; Terabe, S., Sample stacking of cationic and anionic analytes in capillary electrophoresis. *Journal of Chromatography A* **2000**, *902*, 119-135.
7. Hayes, M. A.; Kheterpal, I.; Ewing, A. G., Effects of Buffer pH on Electroosmotic Flow Control by an Applied Radial Voltage for Capillary Zone Electrophoresis. *Anal. Chem* **1993**, *65*, 27-31.
8. Xuan, X.; Li, D., Analytical study of Joule heating effects on electrokinetic transportation in capillary electrophoresis. *Journal of Chromatography A* **2004**, *1064* (2005), 227-237.
9. Chien, R.-L.; Burgi, D. S., Optimization in Sample Stacking for High-Performance Capillary Electrophoresis. *Anal. Chem* **1991**, *63* (18), 2042-2047.
10. Chien, R.-L.; Burgi, D. S., Sample Stacking of an Extremely Large Injection Volume in High-Performance Capillary Electrophoresis. *Anal. Chem* **1992**, *64*, 1046-1050.
11. Quirino, J. P.; Terabe, S., Sample stacking of cationic and anionic analytes in capillary electrophoresis. *Journal of Chromatography A* **2000**, *902* (2000), 119-135.
12. Quin, W., Chemiluminescence Flow-Through Sensor for Copper Based on an Anodic Stripping Voltammetric Flow Cell and an Ion-Exchange Column with Immobilized Reagents. *Anal. Chem* **1998**, *70*, 3579-3584.
13. Chen, Y.; Lin, Z.; Chen, J.; Sun, J.; Zhang, L.; Chen, G. H., New capillary electrophoresis-electrochemiluminescence detection system equipped with an electrically heated Ru(bpy)₃²⁺/multi-wall-carbon-nanotube paste electrode. *J Chromatogr A* **2007**, *1172*.
14. Carr, A.; Dickson, J.; Dickson, M.; Milofsky, R., Post-Column Ultra-Fast Co-Catalyzed Peroxyoxalate Chemiluminescence Detection in Capillary Electrophoresis and Capillary Electrochromatography. *Chromatographia* **2012**, *55*, 687-692.
15. Xu, X.; Li, L.; Weber, S. G., Electrochemical and optical detectors for capillary and chip separations. *Trends in Analytical Chemistry* **2007**, *6* (1).
16. Durgbanshi, A.; K, W. T., Capillary electrophoresis and electrochemical detection with a conventional detector cell. *Journal of Chromatography A* **1998**, *798*, 289-296.
17. Swinney, K.; Bornhop, D. J., Detection in capillary electrophoresis. *Electrophoresis* **2000**, *21*, 1239-1250.
18. Stradiotto, N. R.; Yamanaka, H.; Valnice, M. B. Z., Electrochemical sensors: A powerful tool in analytical chemistry. *J. Braz. Chem. Soc.* **2003**, *14* (2).
19. Dadoo, R.; Seto, A. G.; Colon, L. A.; Zare, R. N., End-Column Chemiluminescence Detector for Capillary Electrophoresis. *Anal. Chem* **1994**, *66*, 303-306.

20. Xu, Q.; Ji, X.; Li, H.; Liu, J.; he, Z., An on-column fracture/end-column reaction interface for chemiluminescence detection in capillary electrophoresis. *Journal of Chromatography* **2010**, *1217*, 5628-5634.
21. Huang, X.; Ren, J., Chemiluminescence detection for capillary electrophoresis and microchip capillary electrophoresis. *Trends in Analytical Chemistry* **2006**, *25* (2).
22. Tsukagoshi, K.; Nakahama, K.; Nakajima, R., Direct Detection of Biomolecules in a Capillary Electrophoresis–Chemiluminescence Detection System. *Anal. Chem* **2004**, *76* (15), 4410-4415.
23. Shah, S. N. A.; Lin, J.-M., Recent advances in chemiluminescence based on carbonaceous dots. *Advances in Colloid and Interface Science* **2017**, *241*, 24-36.
24. Baeyens, W. R. G.; Schulam, S. G.; Calokerinos, A. C.; Zhao, Y.; Campana, A. M. G.; Nakashima, K.; Keukeleire, D. D., Chemiluminescence-based detection: principles and analytical applications in flowing streams and in immunoassays. *Journal of Pharmaceutical and Biomedical Analysis* **1998**, *17*, 941-953.
25. Liu, Y.; Lin, M.; Liu, L.; Peng, L.; Yong-hong, C.; Ren, S., Sensitive Chemiluminescence Immunoassay by Capillary Electrophoresis with Gold Nanoparticles. *Anal. Chem* **2011**, *83*, 1134-1143.
26. Santafe, A. A.-M.; Doumeche, B.; Blum, L. J.; Girard-Egrot, A. P.; Marquette, C. A., 1-Ethyl-3-Methylimidazolium Ethylsulfate/Copper Catalyst for the Enhancement of Glucose Chemiluminescent Detection: Effects on Light Emission and Enzyme Activity. *Journal of Analytical Chemistry* **2010**, *82*, 2401-2404.
27. Zhao, S.; Huang, Y.; Shi, M.; Liu, R.; Liu, Y. M., Chemiluminescence resonance energy transfer-based detection for microchip electrophoresis. *Anal Chem* **2010**, *82* (5), 2036-41.
28. Khan, P.; Idrees, D.; Moxley, M. A.; Corbett, J. A.; Ahmad, F.; von Figura, G.; Sly, W.; Waheed, A.; Hassan, M., Luminol-Based Chemiluminescent Signals: Clinical and Non-clinical Application and Future Uses. *Appl Biochem Biotechnol* **2014**.
29. Bao, J.; Regnier, F. E., Ultramicro enzyme assays in a capillary electrophoretic system. *Journal of Chromatography* **1992**, *608* (1992), 217-224.
30. Yan, C.; Zou, X., 3.13.2 Models for the Mechanisms of Protein Binding. In *Science Direct*, Fig. 2. Schematic diagrams for the three binding models. (A) The lock-and-key model, B. i.-f. m., and (C) conformational-selection model., Ed. 2017.
31. Lineweaver–Burk plot of Michaelis–Menten kinetics. In *Chem.LibreTexts*, LibreTexts: 2020.
32. Michaelis-Menten Kinetics and Briggs-Haldane Kinetics. University of Washington.
33. Gilman, D.; Whisnant, A., Studies of reversible inhibition, irreversible inhibition, and activation of alkaline phosphates by capillary electrophoresis. *Anal Biochem* **2001**, *307* (2002), 226-234.
34. Harmon, B. J.; Patterson, D. H.; Regnier, F. E., Electrophoretically mediated microanalysis of ethanol. *Journal of Chromatography A* **1993**, *657* (1993), 429-434.
35. Patterson, D. H.; Harmon, B. J.; Regnier, F. E., Electrophoretically mediated microanalysis of calcium. *Journal of Chromatography A* **1994**, *662*, 389-395.
36. Gattu, S.; Carihfield, C. L.; Lu, G.; Bwanali, L.; Veltri, L. M.; Holland, L. A., Advances in enzyme substrate analysis with capillary electrophoresis. *Methods* **2018**, *146*, 93-106.
37. Fan, Y.; Scriba, G. K. E., Advances in-capillary electrophoretic enzyme assays. *Journal of Pharmaceutical and Biomedical Analysis* **2010**, *53* (2010), 1076-1090.
38. Bankar, S. B.; Bule, M. V.; Singhal, R. S.; Ananthanarayan, L., Glucose oxidase - An overview *Biotechnology Advances* **2009**, *27*, 489-501.

39. BRENDA: The Comprehensive Enzyme Information System. In *1.1.3.4: glucose oxidase*, Technical University of Braunschwig: 2020.
40. Lineweaver-Burk plot for enzyme inhibition. In *NCBI*.
41. Rogers, M. J.; Brandt, K. G., Multiple Inhibition Analysis of *Aspergillus niger* Glucose Oxidase by n-Glucal and Halide Ions. *Biochemistry* **1971**, *10* (25), 4636-4640.
42. Rogers, M. J.; Brandt, K. G., Interaction of Halide Ions with *Aspergillus niger* Glucose Oxidase. *Biochemistry* **1971**, *10* (25), 4630-4635.
43. Seaton, B., Indirect Determination of Enzyme Kinetics Using Capillary Electrophoresis with Chemiluminescence Detection. Appalachian State University: 2016.

Vita:

GraceAnna (Gracie) Taylor Portagallo was born on July 23rd, 1998 in Middletown, New Jersey. Gracie will be graduating *Cum Laude* from Appalachian State University in May 2021 with a Bachelor of Science in Chemistry and a minor in Physics, as well as Departmental Honors. She will begin her Master's degree in Engineering Physics at Appalachian State University in August 2021.